

# Enhancing Electrochemical Performance of Ni-rich Cathode by Utilizing Organic Anhydride Cathode Additive

Yongkang Han<sup>1</sup>, Yingchuan Zhang<sup>1</sup>, Yike Lei<sup>1</sup>, Jie Ni<sup>1</sup>, Cunman Zhang<sup>1</sup>, Qiangfeng Xiao<sup>1\*</sup>

<sup>1</sup> School of Automotive Studies & Clean Energy Automotive Engineering Center, Tongji University, Shanghai, 201804, PR China

(\*Corresponding Author: xiaoqf@tongji.edu.cn)

## ABSTRACT

Ni-rich  $\text{LiNi}_x\text{Mn}_y\text{Co}_{1-x-y}\text{O}_2$  ( $x \geq 0.8$ ) cathode is widely applied in high-end vehicle for its relatively high specific capacity and operating potential, which receives extensive attention in academia and industry. However, poor cycling performance and high cost hinder its further applications in lithium-ion batteries. In this work, 2-Methylenesuccinic anhydride is utilized as a functional cathode additive. Through the interaction between low valence Ni ions and anhydride, the facile approach allows functional 2-Methylenesuccinic anhydride more precisely work at the interface. As the operation potential rises, 2-Methylenesuccinic anhydride is oxidized prior to the electrolyte and a robust CEI layer rich in carbon oxygen double bond is built in the surface of cathode particles upon cycling, which has been analyzed by TEM and XPS. Besides, 2-Methylenesuccinic anhydride can absorb the trace of water in the cathode and electrolyte. As a result, the 0.5wt% 2-Methylenesuccinic anhydride modified NCM sample retains 91.6 % of initial capacity after charge-discharge 400 cycles at 2C. The novel modification strategy by adding a cathode additive is of important significance for mitigating deleterious side reactions in the interface for Ni-rich NCM materials.

**Keywords:** high energy density cathode, energy storage, lithium ion batteries, organic anhydride, energy systems, Ni-rich cathode materials

## NONMENCLATURE

### Abbreviations

LIBs	Lithium-ion Batteries
MA	2-Methylenesuccinic Anhydride
Ni-rich NCM	$\text{LiNi}_x\text{Mn}_y\text{Co}_{1-x-y}\text{O}_2$ , $x \geq 0.8$

## 1. INTRODUCTION

LIBs are widely used in electric automobile, large energy storage system, portable electronic products, and are moving to high energy density and long life[1-3]. Layered Ni-rich NCM materials are a preferred cathode material for long-range electrical vehicles because of their high capacity ( $>200 \text{ mA h g}^{-1}$ ) and high voltage ( $>3.8 \text{ V}$ ), but it suffers from surface structure degradation, parasitic reaction, moisture sensitivity, and severe gas production[4-6]. Without grain boundaries, single-crystalline Ni-rich materials show great advantages in solving the problems present in its polycrystalline counterpart [7-9]. However, the poor cycle performance and high cost still hinder its further large-scale application in next-generation advanced lithium-ion batteries[10].

The poor cycle performance of single-crystalline NCM cathode is related with the unstable interface [11]. First, surface structure degradation (layered R3m phase  $\rightarrow$  spinel phase  $\rightarrow$  rock-salt Fm3m phase) occurs a on the particle surface during the electrochemical process[12, 13]. The final rock-salt NiO-Like product is a non-electrochemical active rhombohedral phase that will increase interface impedance and aggravate cation mixing. Second, it is well known that the serious parasitic reaction between  $\text{Ni}^{4+}$  and the carbonate electrolytes cannot to be neglected, accompanied by gas generation and increased impedance, which is a crucial cause for the serious capacity decline during cycles[14]. Third, the dissolution of transition metals in electrolytes is an important challenge to improve the electrochemical performance. In addition, Ni-rich NCM cathode is very sensitive to moisture and carbon dioxide when exposed to air, residual lithium ( $\text{Li}_2\text{CO}_3$ ,  $\text{LiHCO}_3$  and  $\text{LiOH}$ ) will be produced during manufacturing and storage process on the surface of NCM material[15, 16]. Beyond that,

Sicklinger *et al.* reported that the removal of Ni<sup>2+</sup> from the crystal lattice can react with the CO<sub>2</sub> and H<sub>2</sub>O to form residual alkali compounds NiCO<sub>3</sub> and Ni(OH)<sub>2</sub> × H<sub>2</sub>O[17]. Jung *et al.* reported earlier the formation of NiCO<sub>3</sub> species, instead of the Li<sub>2</sub>CO<sub>3</sub>, which covered the surface of NCM811 particles while storing in the air [18].

To solve these problems, researchers reported various approaches, focusing on particles engineering, surface modification, doping and electrolyte additives[19]. Among these approaches, adding functional electrolyte additives is a simple and efficient strategy to stabilize the interface of cathode materials, because an amount of functional additive would form a CEI layer covering the surface of electrode through self-sacrifice [20, 21]. However, to develop an electrolyte additive, both positive and negative electrodes must be considered. More importantly, the electrolyte additives are not fully consumed after activation. It is continuously consumed during subsequent electrochemical process, contributing to the continued growth of the interfacial passivation layer. Therefore, more and more researchers began to pay attention to the functional cathode additives that are added into the slurry during the electrode manufacturing process. Li<sub>2</sub>C<sub>2</sub>O<sub>4</sub> has a theoretical capacity of up to 525 mA h g<sup>-1</sup>, its decomposition voltage up to 4.7 V, and it has been successfully applied to LiNi<sub>0.5</sub>Mn<sub>1.5</sub>O<sub>4</sub>/silicon-graphite full battery as cathode additive[22]. By reducing the size and adding NiO catalyst, Huang *et al.* reduced the decomposition potential of Li<sub>2</sub>C<sub>2</sub>O<sub>4</sub> cathode additive and improved the battery performance of LiFePO<sub>4</sub>[23]. However, severe gas production still limits its application. Yang *et al.* reported that LiCoO<sub>2</sub> has a reversible capacity of 170 mA h g<sup>-1</sup> after 200 cycles at 4.6 V after adding aluminum isopropoxide additive during the electrode manufacturing process [24]. By using about 0.25-0.50 wt% sulfur cathode additives, Zhang *et al.* obviously improved rate capability performance of layered NCM811 cathode [25]. Wu *et al.* reported that the full-cell (graphite vs. LiNi<sub>0.8</sub>Co<sub>0.1</sub>Mn<sub>0.1</sub>O<sub>2</sub> cathode) shows an initial charge capacity of up to 277.3 mAh g<sup>-1</sup> initial charge capacity and a conventional discharge capacity of 186.5 mAh g<sup>-1</sup> when using Cu-substituted Li<sub>2</sub>Cu<sub>0.1</sub>Ni<sub>0.9</sub>O<sub>2</sub> as the cathode pre-lithiation additives[26]. Kim *et al.* reported a pre-lithium additive Li<sub>8</sub>ZrO<sub>6</sub> that can compensate for the first cycle lithium loss of the battery[27]. The additives discussed above are not renewable, and Li<sub>2</sub>Cu<sub>0.1</sub>Ni<sub>0.9</sub>O<sub>2</sub> as well as Li<sub>8</sub>ZrO<sub>6</sub> contain rare metals.

It is well known that layered Ni-Rich NCM cathode has a high cost because it is rich in nickel and cobalt. Therefore, simple and efficient modification methods are

avored by industry and researchers. In this work, renewable MA as a cathode additive was added into the slurry in the electrode manufacturing process. On the other hand, the characteristics of the positive side can be utilized by cathode additive to achieve some specific functions. According to previous reports, low valence Ni ions can react with succinic anhydride and methyl succinic anhydride[28]. As mentioned in the second paragraph above that a part of low nickel salts (NiCO<sub>3</sub> and Ni(OH)<sub>2</sub>) are covered in the surface of Ni-rich NCM particles after processing and storage. In this way, it is possible to use low valence Ni ions on the surface of cathode to target the organic anhydride, leading organic anhydride to work more precisely on the interface. As the operation potential rises, MA are oxidized prior to the electrolyte and a robust CEI layer rich in carbon oxygen double bond is built in the surface of cathode particles upon cycling, which is analyzed by TEM and XPS. The robust CEI layer would prevent the serious parasitic reaction and enhance the battery performance of layered Ni-rich NCM materials. Besides, MA can absorb the water trace in the cathode surface and electrolyte, inhibiting the hydrolysis of lithium salts. The novel modification strategy by adding a renewable MA cathode additive is of important significance for mitigating deleterious side reactions in the interface for Ni-rich NCM materials.

## 2. MATERIAL AND METHODS

### 2.1 Preparation of Electrodes

The used Ni-rich NCM811 powder in this experiment was obtained from Li-Fun. 2-Methylenesuccinic anhydride (99%) was purchased from Adamas-beta. The pristine electrodes were prepared, described as follows: Ni-rich NCM, conductive additive SP and binder PVDF with mass ratio of 85:10:5 were dispersed in NMP solvent by balling. Subsequently, the obtained slurry was evenly applied to the aluminum foil by using a 150 μm stainless steel scraper and further dried in a vacuum oven at 80 °C for 12 h. The dry electrodes were drilled into a small disc and the Ni-rich NCM loading is about 3mg cm<sup>-2</sup>. The modified electrodes are different from pristine electrode that adding different amounts of MA during the slurry. The weight ratio between the NCM cathode and the MA was controlled at 100:0, 100:0.5, 100:1.0 and 100:1.5 and the obtained cathodes are denoted as NCM, 0.5%MA, 1.0%MA, and 1.5%MA, respectively. It is worth noting that the modified electrodes need to be dried at 75 °C.

## 2.2 Batteries test

The electrochemical performance was evaluated with a conventional CR2032-type coin cells, which was consisting of a lithium foil anode, porous polypropylene separator (Celgard 2400), NCM cathode and electrolyte. All of the above cells were assembled in the argon-filled glove box ( $O_2 < 0.5$  ppm,  $H_2O < 0.5$  ppm). 1M LiPF<sub>6</sub> (lithium hexafluorophosphate) dissolved in the mixture solvent of EMC (ethyl methyl carbonate) and EC (ethylene carbonate) (7:3 by volume ratio) with 2 wt% VC (vinylene carbonate) additive was used as the electrolyte. The amount of electrolyte used in Li||NCM cells is 45 $\mu$ L.

The electrochemical tests were implemented on a NEWARE workstation (NEWARE CT2001A) at 25 °C in an incubator. Before testing, the cell formation was carried at 0.1 C (20 mA g<sup>-1</sup>) charge/discharge current for three cycles. Subsequently, long cycle performance was conducted at 0.5C or 2C rate between 2.7 and 4.3V. The rate capability was compared at various current density (0.1C, 0.2C, 0.5C, 1C, 2C, 3C, 5C, 10C, 0.1C) with five cycles per each current density.

## 2.3 Material characterization

The bulk structure of NCM cathode were examined by using the X-ray diffraction (XRD, Rigaku Ultimate IV, Japan) with a scan rate of 5°/min from 10° to 80°. The morphologies of samples were obtained by the scanning electron microscope (SEM, Zeiss Sigma 300, Germany). X-ray photoelectron spectroscopy (XPS, Thermo Scientific K-Alpha, USA) was carried out to obtain the surface chemical composition of cathodes after cycles. The morphologies of the CEI film on the cathode surface was obtained by the transmission electron microscope (TEM, JEM2100F, Japan).

## 3. RESULTS AND DISCUSSION

First, the morphologies of pristine NCM, and 0.5% MA sample are obtained by SEM (Fig. 1). The pristine NCM sample shows clear edge and smooth surface with the average particle size of about 2 $\mu$ m. Interestingly, it is observed that some fringes are distributed uniformly on the surface of 0.5% sample, which may be attributed to the reaction between low valence Ni ion and MA that MA-Ni derivatives deposited on the surface of the cathode particle. As expected, no evidences support that the morphologies of cathode were damaged after adding MA into the electrode. After electrochemical cycles, the surface of 0.5% MA particles is smoother and more uniform than that of pristine particles, indicating less side reaction occur on the surface of 0.5%MA particles.

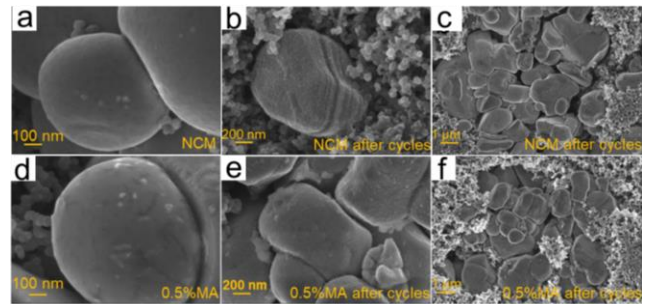


Fig. 1. The SEM of pristine NCM electrode and 0.5%MA electrode before and after cycles

Besides, the bulk structure of electrodes with or without MA were examined by XRD. As is shown in Fig. 2, the XRD patterns of the all samples are indexed to the hexagonal  $\alpha$ -NaFeO<sub>2</sub> structure, belonging to rhombohedral R3m space group[2, 4, 29]. The intensity ratio of (003)/ (104) peaks is over 1.2, suggesting that the undesirable cation mixing is low[30]. More importantly, the clear splitting of (108)/ (110) and (006)/ (102) peaks suggests the highly ordered layered structure, which confirms that the modification process did not break bulk phase structure of NCM material[31].

After three cycles of activation (0.1C), long cycling performance of the Li | NCM cells was evaluated (0.5 C charge and discharge, 1C = 200 mA g<sup>-1</sup>) in the voltage range of 2.7- 4.3 V at 25 °C (Fig. 3a). The cells used the conventional carbonate electrolyte. Compared with the pristine samples, 0.5% MA exhibits slightly higher initial capacity of 182.8 mAh g<sup>-1</sup>. However, adding excess MA such as 1.5% shows sharp decline in initial capacity because excess MA leads to large internal resistance and hinders the transport of lithium ions. A more interesting

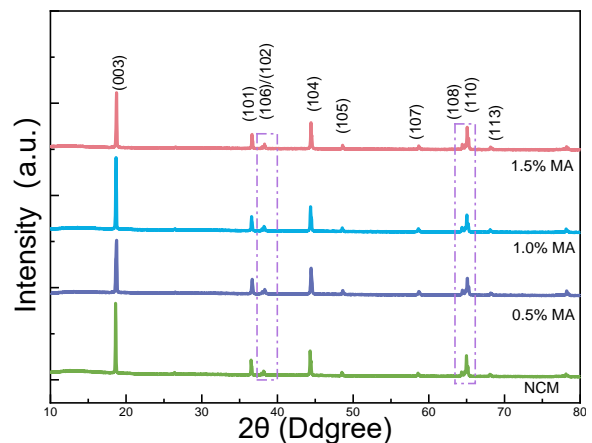


Fig. 2. The XRD results of pristine NCM, 0.5%MA, 1.0%MA and 1.5%MA).

phenomenon is that the capacity of modified samples is increasing during the first 15 cycles. The phenomenon is related with the process that MA are participating in the construction of CEI film. The capacity retention of pristine cathode dropped below 73.2 % at the 200th cycle, while 0.5% MA shows better capacity retention more than 87%. Although the initial capacity is sacrificed, 1%MA and 1.5%MA both have better cycling performance than the pristine NCM sample. These results suggest that adding a suitable amount of MA can improve the electrochemical cycling performance because added MA suppresses side reactions in the interface and preserves a stable electrode-electrolyte interface.

The rate performance was further evaluated with different current density. Fig.3b shows the rate performance for pristine samples and modified sample with MA. At the current density of 0.1C, we observe an increase in the discharge capacity of the modified sample, which is consistent with the previous discussion. As expected, after adding a suitable amount of MA, the electrode exhibits better rate capability than the pristine sample. The improvement with 0.5% MA is shown to be the best. Obviously, the gap between pristine sample and 0.5%MA become larger as the current density increases. At the current density of 10 C, 0.5% MA maintains a discharge capacity of 130.6 mA h g<sup>-1</sup> (66.7%

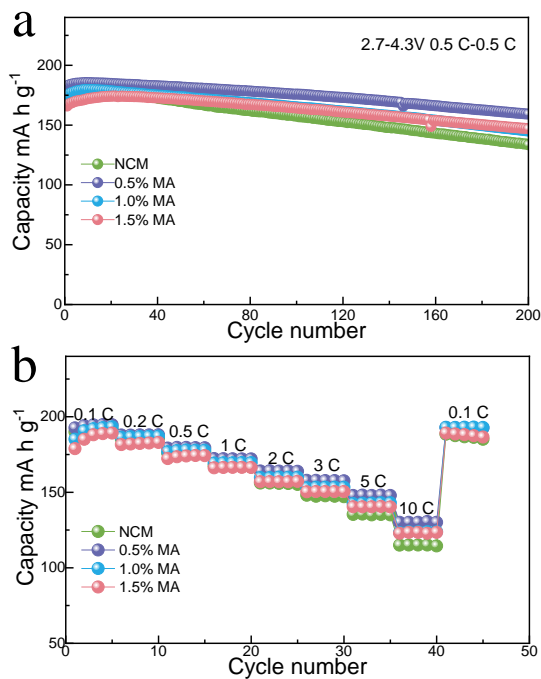


Fig.3. (a) The cycling performance of 0.5%MA, 1.0%MA and 1.5%MA. (b) The rate performance of different samples.

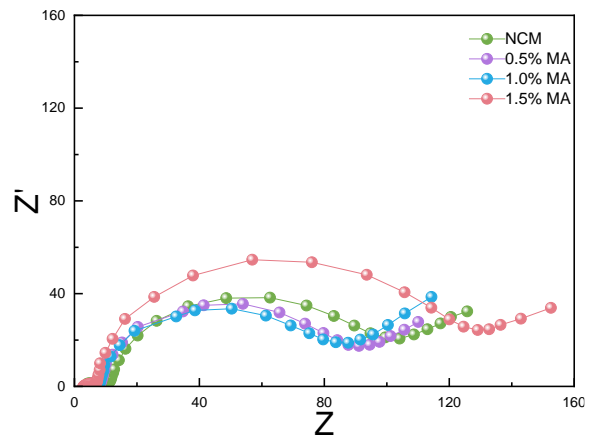


Fig.4. The EIS spectra for the pristine NCM, 0.5%MA, 1.0%MA and 1.5%MA cathode after 200 cycles.

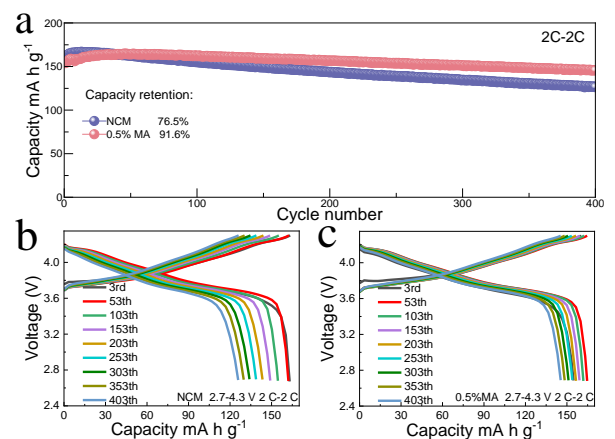


Fig. 5. (a) The high rate cycling performance of pristine NCM, and 0.5%MA. The voltage profiles in different cycles

capacity retention), significantly higher than that of 114.8 mA h g<sup>-1</sup> for the pristine cathode. Excess MA can lead to poor performance at low current density, but the change at high current density is not obvious. The considerable rate performance of modified sample is related to the lower interface resistance of batteries with MA, which is revealed by the EIS results (Fig. 4) for batteries after 200 cycles. Another reason is associated with the stabilized CEI by MA, which can suppress the phase transformation and interfacial parasitic reaction.

After 200 cycles, the EIS spectra for the pristine NCM, 0.5% MA, 1.0% MA and 1.5% MA cathode are compared in Fig. 4. In the EIS spectra, the semicircle at the highest frequency represents the cathode electrolyte interface (R<sub>CEI</sub>), the second semicircle at medium frequency reflects the charge transfer resistance (R<sub>ct</sub>), the sloped line in the low frequency region is the Warburg impedance that is related to diffusion of lithium ions in

the bulk electrode[31, 32]. It is well known that the charge transfer resistance ( $R_{ct}$ ) is the dominant cause of the capacity-fading for Ni-rich NCM cathode. Applying a certain amount of MA, including the 0.5%, 1%, 1.5% MA samples, can reduce  $R_{CEI}$  (all below 10  $\Omega$ ) compared with that of pristine sample, indicating MA has a positive effect on the CEI. However, only adding appropriate amount of MA can reduce the charge transfer resistance  $R_{ct}$ . Adding excess amount of MA, such as 1.5% MA will increase the larger the charge transfer resistance  $R_{ct}$ , because excess MA hinders the transport of lithium ions. Specifically, the  $R_{ct}$  of the cell modified with the 0.5% MA is about 80.2  $\Omega$  after 200 cycles, while the cell that of pristine cathode presents a greater  $R_{ct}$  of 90.5  $\Omega$  under the same condition. The cell of 1.0% MA sample shows a similar large  $R_{ct}$  to that of 0.5%MA. However, the  $R_{ct}$  of 1.5% MA significantly increased to 121.1  $\Omega$  after 200 cycles.

High rate (2C charge and 2C discharge) long cycling performance was further evaluated (Fig. 5a). To reduce the influence of lithium metal, high concentrated salt electrolyte (4M LiFSI/DME based electrolyte) was utilized to obtain the 2C charge and 2C discharge cycling performance. High-concentration electrolytes have attracted extensive attention, because their unusual functionalities significantly improve the interfacial stability between lithium metal anode and electrolyte[33, 34]. At 2C charge and 2C discharge current density, 0.5% MA maintains 91.6% capacity retention after 400 cycles; while the sample without MA additive only shows a capacity retention of 76.5% after 400 cycles. Fig. 5b, c shows the voltage profiles in selected cycles for pristine NCM and 0.5%MA. The 0.5% MA battery shows a unobvious increase of overpotential and polarization during electrochemical process, indicating superior high rate cycling stability because of the protection of robust CEI layer. As a contrary, the pristine sample shows the opposite phenomenon with continuous capacity decay, which was mainly associated with unstable interfaces and serious parasitic reactions.

It is indispensable to analyze the morphology and composition of CEI because good CEI layer on the cathode plays a determinative role in protecting the cathode surface, inhibiting the side reaction and improving the interface stability. As is shown in Fig.6a,b, a uneven and thick CEI film covers on the pristine cathode surface after 100 cycles; while the CEI of 0.5% MA cathode surface is uniform and thin, suggesting less side reactions occur at the interface of the modified sample. Not only that, the dense CEI inhibits irreversible phase transition (layered R3m phase  $\rightarrow$  spinel phase  $\rightarrow$

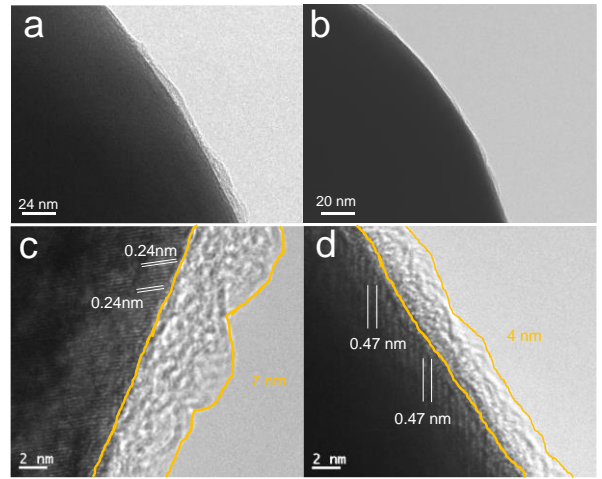


Fig. 6. HRTEM images of (a, c) pristine cathode and (b, d) 0.5% MA cathode after 100 cycles.

rock-salt Fm3m phase) on the surface of the cathode particles[13]. Therefore, Fig. 6c exhibits obvious lattice fringe (The lattice spacing  $d=0.24$  nm) that is assigned to rock-salt Fm3m structure, attributing to its continuous surface degradation on the cathode surface. In contrast, the surface of cycled 0.5% MA particle shows layered R3m phase ( $d=0.47$  nm) in Fig. 6d because of comprehensive protection of excellent CEI film.

XPS was utilized to analyze the chemical composition of CEI on the cathode surface. Fig. 7 displays the XPS spectra of the pristine NCM and 0.5% MA samples after 100 cycles. As shown in Fig.7a, b, the O 1s spectra of the

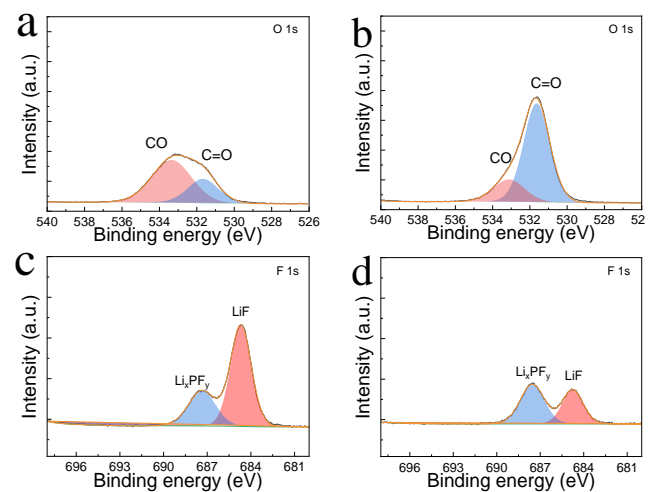


Fig. 7. XPS spectra of (a) O1s, and (c) F 1s for pristine NCM cathode after 100 cycles. XPS spectra of (b) O 1s and (d) F 1s for 0.5% MA electrode after 100 cycles.

cycled pristine cathode and 0.5% MA cathode present main two peaks, which are attributed to the CO<sup>-</sup> (533.2V) and C=O (532.0 eV). As expected, the modified sample with MA shows more obvious carbon-oxygen double bond signal in the CEI layer after cycling, which is derived from MA. MA is an important Itaconic acid derivative and fine chemical raw material because its molecules contain carbon-carbon unsaturated double bonds and anhydride groups. The results suggest that the introduced anhydride can accurately act on the interface to produce CEI with a part of inherited anhydride properties. In comparison, the C-O peaks in the CEI of MA-contained sample are much weaker than that of the pristine NCM cathode, indicating CEI rich in carbon-oxygen restrain continuous side reaction the carbonate electrolyte and the cathode. Li<sub>x</sub>PF<sub>y</sub> (688.8 eV) and LiF (684.8 eV) peaks are present in the F 1s spectra (Fig. 7c, d), which is attributed to the LiPF<sub>6</sub> decomposition. LiF is the main by-product in the CEI when LiPF<sub>6</sub> is used as lithium salt in carbonate electrolyte, and LiF is derived mainly from the thermal decomposition (LiPF<sub>6</sub> → LiF + PF<sub>5</sub>) and hydrolysis (LiPF<sub>6</sub> + H<sub>2</sub>O → LiF + 2HF + POF<sub>3</sub>) of LiPF<sub>6</sub>. As is shown in Fig. 7c, d, the LiF peaks in the CEI of MA-contained sample are much weaker than that of the pristine NCM cathode. Compared with the pristine NCM, the CEI of 0.5% MA sample shows weaker Li<sub>x</sub>PF<sub>y</sub> and LiF peaks, suggesting that less thermal decomposition and hydrolysis of LiPF<sub>6</sub> occur during the cycles. For one thing, the robust CEI film can inhibit interfacial side reactions between electrodes and electrolyte. For another important thing, the anhydride can capture the water trace in the electrolyte and further inhibit the hydrolysis of lithium salt.

Cyclic voltammetry (CV) and Linear scan voltammetry (LSV) were carried to further research the film forming process of CEI. Firstly, we analyze the charge-discharge curves of the first three cycles of activation at 0.1C. As is shown in Fig. 8a, adding excess MA will increase polarization and reduce the capacity of the battery. Fig. 8b, c shows cyclic voltammetry (CV) curves of pristine cathode and 0.5% MA. By analyzing the CV of the initial cycle, we can obtain the information of CEI film formation and activation process. At the initial CV cycle (Fig. 8b), similar as layered LiNiO<sub>2</sub>, pristine NCM811 experience a tertiary phase transitions corresponding to a tertiary redox reactions, hexagonal (H1) and monoclinic (M), monoclinic and hexagonal (H2), as well as hexagonal and hexagonal (H3) [24]. Nevertheless, the initial CV cycle of 0.5% MA is different to that of pristine NCM sample, that the oxidation peak (hexagonal to monoclinic) moves to a higher potential range obviously and a weak peak appears near 4.1V (Fig.

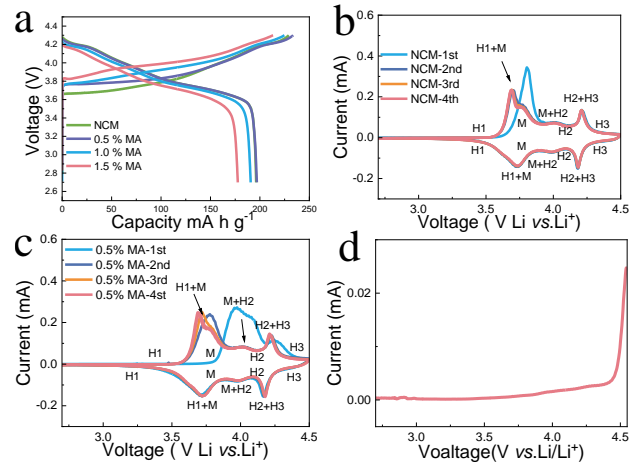


Fig. 8. (a) The initial charging/discharging profiles of pristine NCM, 0.5%MA, 1.0%MA and 1.5% MA. CV curves of (b) pristine NCM and (c) 0.5%MA. (d) LSV of the electrode.

8c). Moreover, we found a significant oxidation curve in the range greater than 4.25V. These indicate that MA is oxidized to form CEI at high voltage to substitute for the decomposition of the electrolyte. The functions of MA are similar a sacrificial electrolyte additive and can work more precisely at the interface. To further prove this, the MA electrode (MA, SP and PVDF with mass ratio of 80:10:10) were prepared, and Li-metal was utilized as counter electrode to assemble a half-cell. Subsequently, LSV was applied with the scanning rate: 0.03 mV s<sup>-1</sup> to evaluate the oxidation stability of MA. In Fig. 8d, we observe a weak oxidation within the voltage range above 4.0 V, which is consist with CV curves.

#### 4. CONCLUSION

In summary, MA was used as a cathode additive for Ni-rich NCM cathode. Through the interaction between low valence Ni ions and anhydride, the facile approach allows functional MA more precisely work at the interface comparing with conventional electrolyte addition. As the operation potential rises, MA are oxidized prior to the electrolyte and a robust CEI layer rich in carbon oxygen double bond is built in the surface of cathode particles upon cycling, which is analyzed by TEM and XPS. As a result, the capacity retention of the 0.5wt% MA modified NCM cathode retains 91.6 % of initial capacity after charge-discharge 400 cycles at 2C. The novel strategy by adding a cathode additive is of important significance for mitigating deleterious side reactions in the interface for Ni-rich cathode materials.

## ACKNOWLEDGEMENT

We acknowledge the financial support provided by the National Natural Science Foundation of China (Grant No. 52073215).

## DECLARATION OF INTEREST STATEMENT

The authors declare that they have no known competing financial interests or personal relationships that could have appeared to influence the work reported in this paper. All authors read and approved the final manuscript.

## REFERENCE

[1] Wang C, Wang R, Huang Z, Chu M, Ji W, Chen Z, et al. Unveiling the migration behavior of lithium ions in NCM/Graphite full cell via in operando neutron diffraction. *Energy Stor Mater*. 2022;44:1-9.

[2] Zhang X, Qiu Y, Cheng F, Wei P, Li Y, Liu Y, et al. Realization of a High-Voltage and High-Rate Nickel-Rich NCM Cathode Material for LIBs by Co and Ti Dual Modification. *ACS Appl Mater Interfaces*. 2021;13:17707-16.

[3] Teichert P, Jahnke H, Figgemeier E. Degradation Mechanism of Monocrystalline Ni-Rich Li[NixMnyCoz]O<sub>2</sub> (NMC) Active Material in Lithium Ion Batteries. *J Electrochem Soc*. 2021;168:090532.

[4] Zhang B, Shen J, Wang Q, Hu C, Luo B, Liu Y, et al. Boosting high-voltage and ultralong-cycling performance of single-crystal LiNi<sub>0.5</sub>Co<sub>0.2</sub>Mn<sub>0.3</sub>O<sub>2</sub> cathode materials via three-in-one modification. *Energy Environ Mater*. 2021;6:e12270.

[5] Han Y, Jung SH, Kwak H, Jun S, Kwak HH, Lee JH, et al. Single- or Poly-Crystalline Ni-Rich Layered Cathode, Sulfide or Halide Solid Electrolyte: Which Will be the Winners for All-Solid-State Batteries? *Adv Energy Mater*. 2021;11:2100126.

[6] Bi Y, Tao J, Wu Y, Li L, Xu Y, Hu E, et al. Reversible planar gliding and microcracking in a single-crystalline Ni-rich cathode. *Science*. 2020;370:1313-7.

[7] Qian G, Li Z, Meng D, Liu J-b, He Y-S, Rao Q, et al. Temperature-Swing Synthesis of Large-Size Single-Crystal LiNi<sub>0.6</sub>Mn<sub>0.2</sub>Co<sub>0.2</sub>O<sub>2</sub> Cathode Materials. *J Electrochem Soc*. 2021;168:010534.

[8] Wang Y, Wang E, Zhang X, Yu H. High-Voltage "Single-Crystal" Cathode Materials for Lithium-Ion Batteries. *Energy & Fuels*. 2021;35:1918-32.

[9] Wang C, Zhang R, Siu C, Ge M, Kisslinger K, Shin Y, et al. Chemomechanically Stable Ultrahigh-Ni Single-Crystalline Cathodes with Improved Oxygen Retention and Delayed Phase Degradations. *Nano Lett*. 2021;21:9797-804.

[10] Li W, Dolocan A, Oh P, Celio H, Park S, Cho J, et al. Dynamic behaviour of interphases and its implication on high-energy-density cathode materials in lithium-ion batteries. *Nat Commun*. 2017;8:14589.

[11] Fan X, Ou X, Zhao W, Liu Y, Zhang B, Zhang J, et al. In situ inorganic conductive network formation in high-voltage single-crystal Ni-rich cathodes. *Nat Commun*. 2021;12:5320.

[12] Liu X, Xu GL, Yin L, Hwang I, Li Y, Lu L, et al. Probing the Thermal-Driven Structural and Chemical Degradation of Ni-Rich Layered Cathodes by Co/Mn Exchange. *J Am Chem Soc*. 2020;142:19745-53.

[13] Yan P, Zheng J, Zhang JG, Wang C. Atomic Resolution Structural and Chemical Imaging Revealing the Sequential Migration of Ni, Co, and Mn upon the Battery Cycling of Layered Cathode. *Nano Lett*. 2017;17:3946-51.

[14] Park SY, Park S, Lim HY, Yoon M, Choi JH, Kwak SK, et al. Ni-Ion-Chelating Strategy for Mitigating the Deterioration of Li-Ion Batteries with Nickel-Rich Cathodes. *Adv Sci*. 2023;10:2205918.

[15] Zhang SS, Ma L. Oxalic Acid as a Cathode Additive Increasing Rate Capability of Ni-Rich Layered Cathode Materials. *J Electrochem Soc*. 2021;168:080512.

[16] Shi JL, Qi R, Zhang XD, Wang PF, Fu WG, Yin YX, et al. High-Thermal- and Air-Stability Cathode Material with Concentration-Gradient Buffer for Li-Ion Batteries. *ACS Appl Mater Interfaces*. 2017;9:42829-35.

[17] Johannes Sicklinger MM, Hans Beyer, Daniel Pritzl, and Hubert A. Gasteiger. Ambient Storage Derived Surface Contamination of NCM811 and NCM111: Performance Implications and Mitigation Strategies. *J Electrochem Soc*. 2019;166:A2322-A35.

[18] Roland Jung RM, Pinar Karayaylali, Katherine Phillips, Filippo Maglia, Christoph Stinner, Yang Shao-Horn, and Hubert A. Gasteiger. Effect of Ambient Storage on the Degradation of Ni-Rich Positive Electrode Materials (NMC811) for Li-Ion Batteries. *J Electrochem Soc*. 2018;165:A132-A41.

[19] Han Y, Lei Y, Ni J, Zhang Y, Geng Z, Ming P, et al. Single-Crystalline Cathodes for Advanced Li-Ion Batteries: Progress and Challenges. *Small*. 2022;18:e2107048.

[20] Zou Y, Liu G, Zhou K, Zhang J, Jiao T, Zhang X, et al. Enhanced Interfacial Stability of a LiNi<sub>0.9</sub>Co<sub>0.05</sub>Mn<sub>0.05</sub>O<sub>2</sub> Cathode by a Diboron Additive. *ACS Appl Energy Mater*. 2021;4:11051-61.

[21] Song W, Harlow J, Logan E, Hebecker H, Coon M, Molino L, et al. A Systematic Study of Electrolyte Additives in Single Crystal and Bimodal LiNi<sub>0.8</sub>Mn<sub>0.1</sub>Co<sub>0.1</sub>O<sub>2</sub>/Graphite Pouch Cells. *J Electrochem Soc*. 2021;168:090503.

[22] Sophie Solchenbach MW, Daniel Pritzl, K. Uta Schwenke, and Hubert A. Gasteiger. Lithium Oxalate as Capacity and Cycle-Life Enhancer in LNMO/Graphite and LNMO/SiG Full Cells. *J Electrochem Soc.* 2018;165:A512-A24.

[23] Huang G, Liang J, Zhong X, Liang H, Cui C, Zeng C, et al. Boosting the capability of Li<sub>2</sub>C<sub>2</sub>O<sub>4</sub> as cathode prelithiation additive for lithium-ion batteries. *Nano Res.* 2023;16:3872-8

[24] Yang J, Liu X, Wang Y, Zhou X, Weng L, Liu Y, et al. Electrolytes Polymerization-Induced Cathode-Electrolyte-Interphase for High Voltage Lithium-Ion Batteries. *Adv Energy Mater.* 2021;11:2101956.

[25] Sheng S, Zhang JC, and Chunsheng Wang. Elemental Sulfur as a Cathode Additive for Enhanced Rate Capability of Layered Lithium Transition Metal Oxides. *J Electrochem Soc.* 2019;164:A487-A92

[26] Wu Y, Zhang W, Li S, Wen N, Zheng J, Zhang L, et al. Li<sub>2</sub>Cu<sub>0.1</sub>Ni<sub>0.9</sub>O<sub>2</sub> with Copper Substitution: A New Cathode Prelithiation Additive for Lithium-Ion Batteries. *ACS Sustain Chem Eng.* 2023;11:1044-53.

[27] Kim M, Spindler BD, Dong L, Stein A. Li<sub>8</sub>ZrO<sub>6</sub> as a Pre-lithiation Additive for Lithium-Ion Batteries. *ACS Applied Energy Materials.* 2022;5:14433-44.

[28] Lin T, Gu Y, Qian P, Guan H, Walsh PJ, Mao J. Nickel-catalyzed reductive coupling of homoenolates and their higher homologues with unactivated alkyl bromides. *Nat Commun.* 2020;11:5638.

[29] Han Y, Xu J, Wang W, Long F, Qu Q, Wang Y, et al. Implanting an electrolyte additive on a single crystal Ni-rich cathode surface for improved cycleability and safety. *J Mater Chem A.* 2020;8:24579-89.

[30] Sun G, Yin X, Yang W, Song A, Jia C, Yang W, et al. The effect of cation mixing controlled by thermal treatment duration on the electrochemical stability of lithium transition-metal oxides. *Phys Chem Chem Phys.* 2017;19:29886-94.

[31] Xu S, Du C, Xu X, Han G, Zuo P, Cheng X, et al. A Mild Surface Washing Method Using Protonated Polyaniline for Ni-rich LiNi<sub>0.8</sub>Co<sub>0.1</sub>Mn<sub>0.1</sub>O<sub>2</sub> Material of Lithium Ion Batteries. *Electrochim Acta.* 2017;248:534-40.

[32] Lei Y, Zhang Y, Han Y, Ni J, Zhang C, Xiao Q. Oxygen-deficient TiO<sub>(2-x)</sub> interlayer enabling Li-rich Mn-based layered oxide cathodes with enhanced reversible capacity and cyclability. *RSC Adv.* 2023;13:16850-9.

[33] Ren X, Chen S, Lee H, Mei D, Engelhard MH, Burton SD, et al. Localized High-Concentration Sulfone Electrolytes for High-Efficiency Lithium-Metal Batteries. *Chem.* 2018;4:1877-92.

[34] Chen S, Zheng J, Mei D, Han KS, Engelhard MH, Zhao W, et al. High-Voltage Lithium-Metal Batteries Enabled

by Localized High-Concentration Electrolytes. *Adv Mater.* 2018;30:1706102.